

---

# A Final Focus Spot Model for Heavy Ion Fusion Driver System Codes\*

**John J. Barnard<sup>1</sup>, Roger O. Bangerter<sup>2</sup>, Enrique Henestroza<sup>2</sup>,  
Igor D. Kaganovich<sup>3</sup>, Edward P. Lee<sup>2</sup>, B. Grant Logan<sup>2</sup>, Wayne  
R. Meier<sup>1</sup>, David Rose<sup>4</sup>, Parthiban Santhanam<sup>2</sup>, William M.  
Sharp<sup>1</sup>, Dale R. Welch<sup>4</sup>, Simon S. Yu<sup>2</sup>**

- 1. Lawrence Livermore National Laboratory**
- 2. Lawrence Berkeley National Laboratory, Livermore**
- 3. Princeton Plasma Physics Laboratory**
- 4. Mission Research Corporation**

**15th International Symposium on Heavy  
Ion Inertial Fusion**

**Princeton University, Princeton, NJ**

**June 7-11, 2004**

Work performed under the auspices of the U.S. Department of Energy under University of California contract W-7405-ENG-48 at LLNL, University of California contract DE-AC03-76SF00098 at LBNL, and contract DEFG0295ER40919 at PPPL.

**The Heavy Ion Fusion Virtual National Laboratory**



# Outline of talk

---

## I. Final focal spot model : Introduction

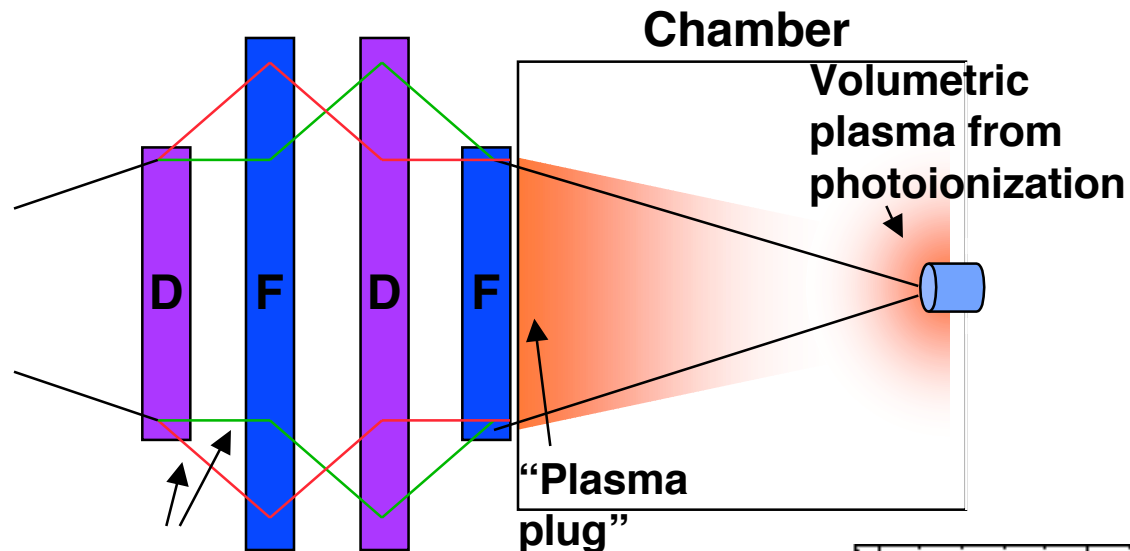
- Incorporated into W. Meier's IBEAM system code
- Need simple enough model to quickly calculate focal spot for large variation in system and beam parameters
- Should be considered status report -- many areas to be improved
- Illustrates research that has gone on into final focus and chamber transport

## II. Physics of final focal spot systems model

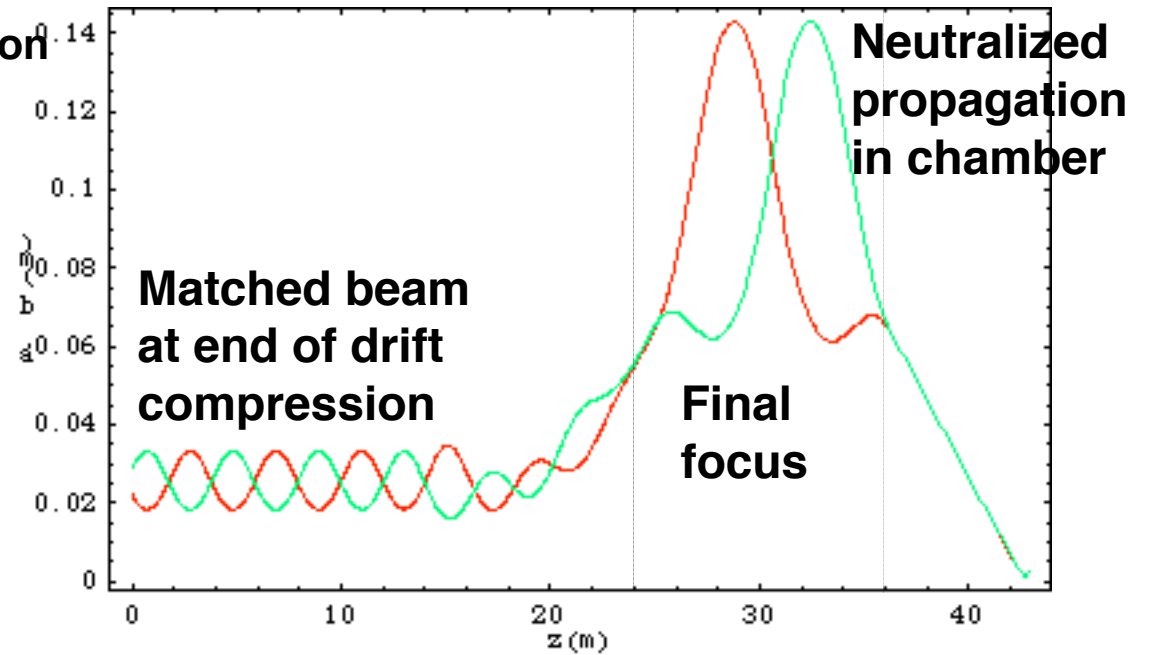
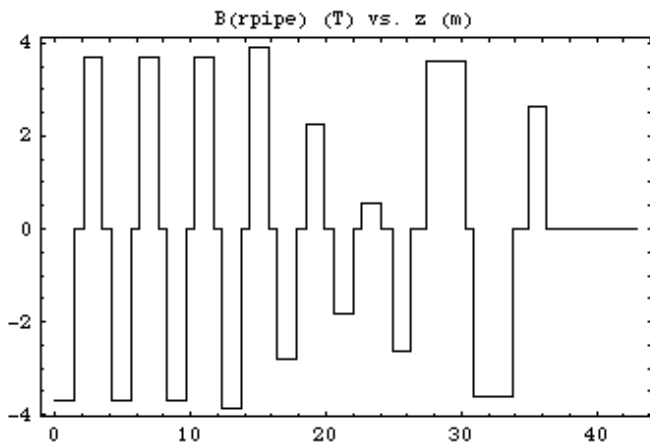
- Emittance
- Chromatic aberrations
- Geometric aberrations
- Space charge
- Neutralized ballistic transport

## III. Example: Robust point design

# To focus the beam to a small spot, the beam radius is first expanded, then compressed and neutralized



x and y envelopes (schematically depicted)



# A simple estimate of spot size can be obtained from the envelope equation

In the chamber the focusing field is absent and the beam can be circular with radius  $a$ :

$$\frac{d^2 a}{dz^2} = \frac{Q}{a} + \frac{\epsilon_x^2}{a^3} \quad \square \quad a^2 \square 2Q \ln a \square \frac{\epsilon_x^2}{a^3} = \text{const.}$$

$$Q = \text{Perveance} \square \frac{\square}{4\square\square_0 V} = \frac{\text{space charge potential}}{\text{ion kinetic energy}}$$

$$\epsilon_x = \text{emittance}$$

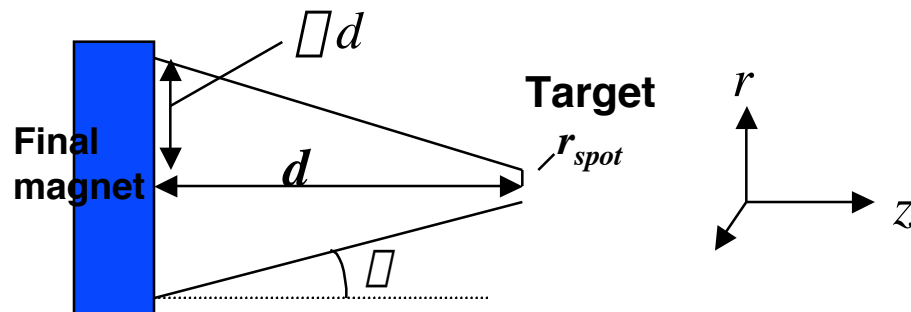
$$a = \text{beam envelope}$$

After exit from final magnet:  $a \square \square\square$ ;  $a = \square d$ ;

At target:  $a \square 0$ ;  $a = r_{spot}$ ;

So energy integral yields:  $\square^2 \square \frac{\epsilon_x^2}{r_{spot}^2} + 2Q \ln \frac{\square d \square}{r_{spot} \square}$  Rearranging ||

$$r_{spot}^2 \square \frac{\epsilon_x^2}{\square^2 \square 2Q \ln \frac{\square d \square}{r_{spot} \square}}$$



So emittance and space charge increase spot radius.  $\square$  requires optimization.

To complete estimate: need  $\square$  from all sources,  $Q$

# The beam will have accumulated both emittance and momentum spread as it enters final focus section

From injector:

Emittance assumed temperature limited (at 1 eV), and size constrained by voltage breakdown limits

Momentum spread dominated by injector voltage ripple, assumed to be of order 0.1 %

Throughout accelerator:

Emittance grows from magnetic field imperfections (assumed at ~0.1% level)

Momentum spread grows from (~1% voltage) errors at induction gaps

$$\sigma_{nxi} = \sigma_{nyi} = 2(kT / mc^2)^{1/2} r_{inj}$$

$$\sigma_{nxq}^2 = \sum_i 4a^2 Q^2 \frac{B_q^2}{B_q^2}$$

$$\sigma_{p_a}^2 = \left(\frac{l_I}{l_a}\right)^2 \sigma_{p_I}^2 + (1/l_a)^2 \sum_i \sigma_{p_i}^2 l_i^2$$

$$\frac{\sigma_{p_a}^2}{p_a^2} = \frac{1}{4V_a^2 t_a^2} \sum_i N_i^2 t_i^2 + \sum_i \frac{N_{pulsar}}{V_{pulsar}} V_{pulsar} L \frac{dV}{ds} t_i^2$$

Model still needs to account for perpendicular-to-parallel energy transfer and other sources of phase space dilution

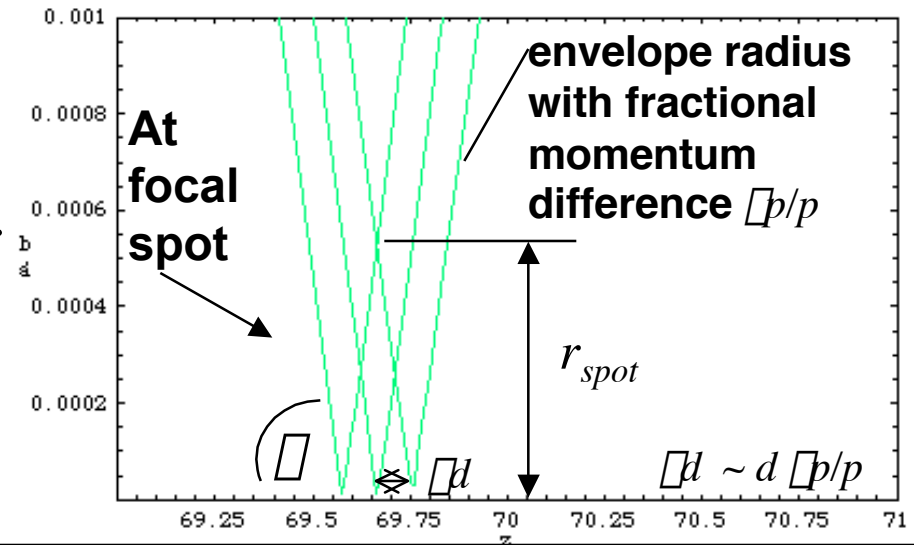
# Chromatic and geometric aberrations are the lowest order corrections to “linearized” transport

“**Chromatic aberrations**” arise because focusing strength of quadrupoles depend on velocity  $v$  (and fractional deviation from design momentum  $\Delta p/p$ ).

$$x'' + K_{xx}x + K_{xx1}x \Delta p/p$$

Different velocity ions come to a focal spot at different distances  $d$

$$r_{spot} \propto C \Delta d (\Delta p/p)$$



“**Geometric aberrations**” arise because

quadrupoles are  $z$ -dependent (i.e. have fringe fields):  $B_{q(r)}(r,z) = B_q(z)r \cos 2\phi$ ;  
Maxwell’s equations require non-linear components:

$$z\text{-component: } B_{(z)} = (1/2)(dB_q/dz)r^2 \cos 2\phi;$$

$$\text{“pseudo-octupole”}: B_{pseudo-oct(r)} = -(1/6)(d^2B_q/dz^2)r^3 \cos 2\phi$$

Also because motion is not purely “paraxial” ( $\Delta^2 = \Delta_z^2(1 + x'^2 + y'^2)$ )

Non-linear terms (3rd order in  $x,y, x',y'$ ) arise in the equations of motion, so expect  $\Delta r_{spot} \sim x'^3 \sim \Delta^3$

# How can we estimate the coefficient for chromatic aberrations?

We constructed moment models to study chromatic effects (through 2nd order) in final focus system

$$\frac{dp_x}{dt} = q(E_x + v_z B_y - v_y B_z)$$

Expand through 2nd order in  $x', y', k_{x0}, k_{y0}, \Delta p/p$

$$x'' + \frac{1}{\beta_z} \frac{d}{dz} (\beta_z) x' - \frac{qB}{m v_z} x' - \frac{\Delta p}{p} + \frac{q}{4\beta_0 m v_z^2} \frac{(x - \bar{x})(1 - \frac{2\Delta p}{p})}{(\beta_x^2 + \beta_y^2)^{1/2}}$$

The equation of motions can be written (where  $\Delta = \Delta p/p$ ):

$$x'' + K_{xx}x + K_{xx1}x\Delta \quad y'' + K_{yy}y + K_{yy1}y\Delta$$

Here:

$$K_{xx} = \frac{B}{[B\Delta]_0} + \frac{Q}{2(\beta_x^2 + \beta_y^2)^{1/2}} \quad K_{yy} = \frac{\beta_x B}{[B\Delta]_0} + \frac{Q}{2(\beta_y^2 + \beta_x^2)^{1/2}}$$

$$K_{xx1} = \frac{\beta_x B}{[B\Delta]_0} + \frac{2Q}{2(\beta_x^2 + \beta_y^2)^{1/2}} \quad K_{yy1} = \frac{\beta_y B}{[B\Delta]_0} + \frac{2Q}{2(\beta_y^2 + \beta_x^2)^{1/2}}$$

$B\Delta$  = quadrupole gradient;  $[B\Delta] =$  Ion rigidity =  $p/q$ ;  $Q =$  perveance =  $\frac{q}{2\beta_0^3 m v_z^2}$

# We take averages of 2nd, 3rd,... order quantities, forming infinite set of 1st order ode's

$\frac{d}{ds} \langle x^2 \rangle = 2 \langle xx \rangle$ $\frac{d}{ds} \langle xx \rangle = \langle x^2 \rangle + \langle xx \rangle$ $= \langle x^2 \rangle + K_{xx} \langle x^2 \rangle + \underline{K_{xx1} \langle x^2 \rangle}$ $\frac{d}{ds} \langle x^2 \rangle = 2 \langle x \rangle$ $= 2 K_{xx} \langle xx \rangle + \underline{2 K_{xx1} \langle xx \rangle}$	$\frac{d}{ds} \langle x^2 \rangle = 2 \langle xx \rangle$ $\frac{d}{ds} \langle xx \rangle = \langle x^2 \rangle + \langle xx \rangle$ $= \langle x^2 \rangle + K_{xx} \langle x^2 \rangle + \underline{K_{xx1} \langle x^2 \rangle}$ $\frac{d}{ds} \langle x^2 \rangle = 2 \langle x \rangle$ $= 2 K_{xx} \langle xx \rangle + \underline{2 K_{xx1} \langle xx \rangle}$	
<p>...</p>	$\frac{d}{ds} \langle x^2 \rangle^n = 2 \langle xx \rangle^n$ $\frac{d}{ds} \langle xx \rangle^n = \langle x^2 \rangle^n + \langle xx \rangle^n$ $= \langle x^2 \rangle^n + K_{xx} \langle x^2 \rangle^n + \underline{K_{xx1} \langle x^2 \rangle^{n+1}}$ $\frac{d}{ds} \langle x^2 \rangle^n = 2 \langle x \rangle^n$ $= 2 K_{xx} \langle xx \rangle^n + \underline{2 K_{xx1} \langle xx \rangle^{n+1}}$	<p><b>⇒ term higher order by one</b></p>



# Infinite set of equations can be truncated, but set is reliable over only finite distances

Two equivalent methods of truncation have been employed:

1.  $\langle x^2 \epsilon^2 \rangle \approx \langle x^2 \rangle \langle \epsilon^2 \rangle$  and  $\langle xx \epsilon^2 \rangle \approx \langle xx \rangle \langle \epsilon^2 \rangle$  ; or
2. Noticing that  $\frac{1}{1+\epsilon} = 1 - \epsilon + \epsilon^2 - \dots$  and  $\frac{1}{1-\epsilon} = 1 + \epsilon + \epsilon^2 + \dots$  thus,

$$\frac{1}{1-\epsilon} \approx \frac{1}{1+\epsilon} = 2\epsilon + 2\epsilon^3 + \dots \quad \text{also} \quad \frac{\epsilon}{1+\epsilon} = \epsilon - \frac{\epsilon^2}{1+\epsilon}$$

so that we may, to good approximation, write

$$\frac{d}{ds} \langle x^2 \rangle = 2 \langle xx \rangle \quad \frac{d}{ds} \langle xx \rangle = \langle x \dot{x}^2 \rangle + K_{xx} \langle x^2 \rangle + \frac{K_{xx1}}{2} \left\langle \frac{x^2}{1-\epsilon} \right\rangle - \left\langle \frac{x^2}{1+\epsilon} \right\rangle + O(x^2 \epsilon^3)$$

$$\frac{d}{ds} \langle x \dot{x}^2 \rangle = 2K_{xx} \langle xx \rangle + K_{xx1} \left\langle \frac{xx \epsilon}{1-\epsilon} \right\rangle - \left\langle \frac{xx \epsilon}{1+\epsilon} \right\rangle + O(xx \epsilon^3)$$

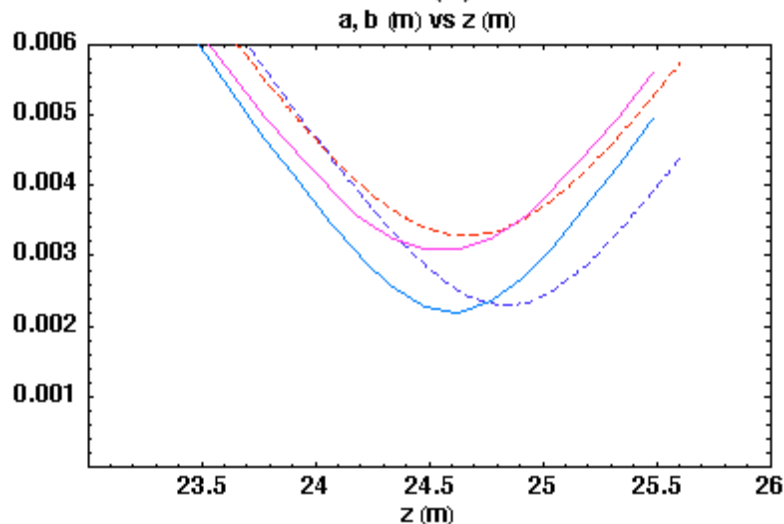
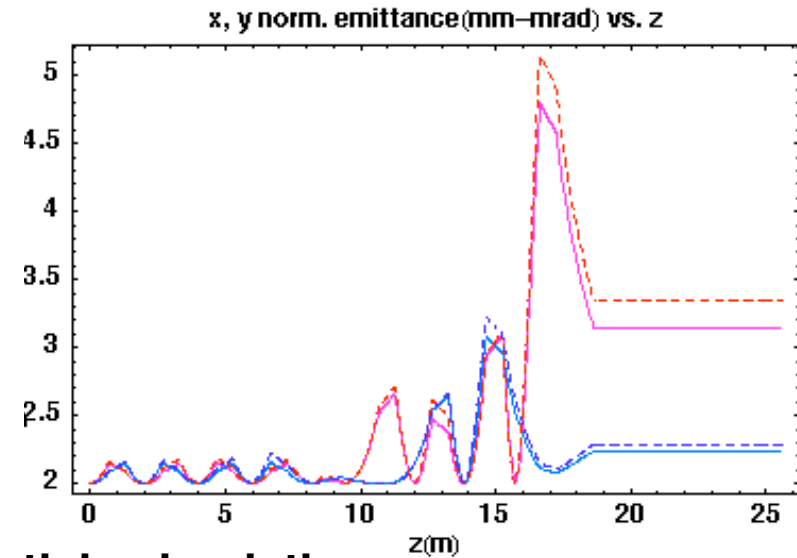
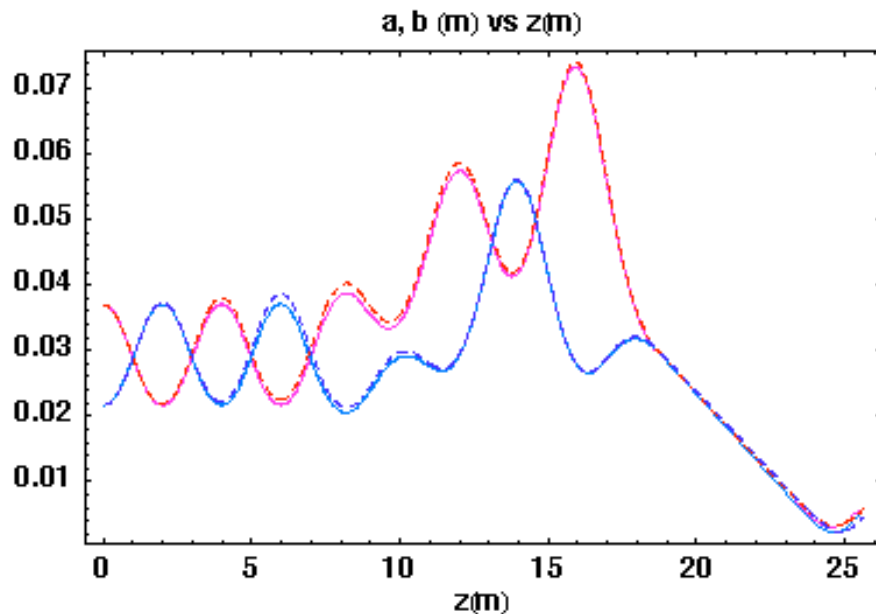
$$\frac{d}{ds} \left\langle \frac{xx \epsilon}{1+\epsilon} \right\rangle = \left\langle \frac{x \dot{x}^2 \epsilon}{1+\epsilon} \right\rangle + K_{xx} \left\langle \frac{x^2 \epsilon}{1+\epsilon} \right\rangle - K_{xx1} \left\langle \frac{x^2 \epsilon}{1-\epsilon} \right\rangle + K_{xx1} \langle x^2 \rangle \quad \frac{d}{ds} \left\langle \frac{x^2}{1+\epsilon} \right\rangle = 2 \left\langle \frac{xx \epsilon}{1+\epsilon} \right\rangle$$

$$\frac{d}{ds} \left\langle \frac{x \dot{x}^2}{1+\epsilon} \right\rangle = 2K_{xx} \left\langle \frac{xx \epsilon}{1+\epsilon} \right\rangle + 2K_{xx1} \langle xx \rangle - 2K_{xx1} \left\langle \frac{xx \epsilon}{1+\epsilon} \right\rangle$$

**Truncated set of equations forms closed set.**

both methods give nearly identical results for  $\epsilon^2$  in the regime of interest; similar equations for  $\langle x^2/(1-\epsilon) \rangle$ ,  $\langle xx \epsilon/(1-\epsilon) \rangle$ ,  $\langle x \dot{x}^2 \epsilon/(1-\epsilon) \rangle$ , and the same set for y; 18 equations total.

# Comparison of moment equations with Particle-in-Cell (WARP) simulations (1% velocity spread)



**Particle simulations:**  
 Dashed, red (x) and blue (y)  
 Initial distribution: KV

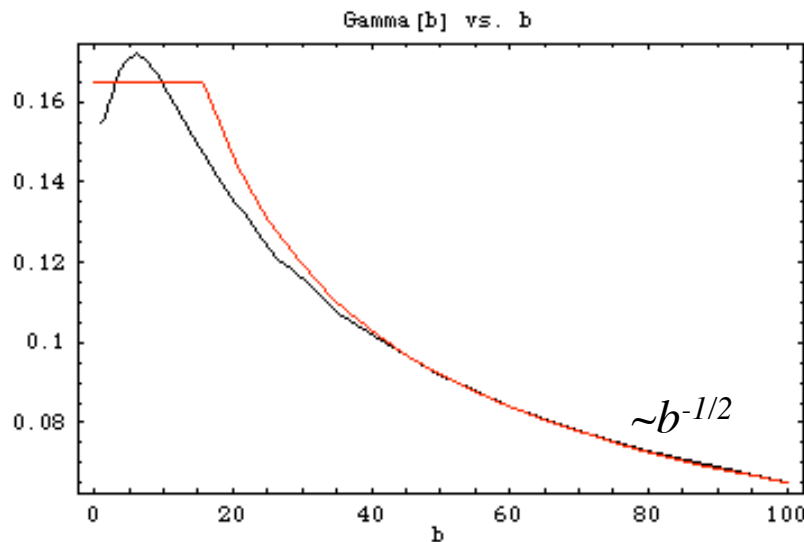
**Moment calculations:**  
 Solid, magenta (x), and aqua (y)

**Result:**

$$\sigma_{cx} = 4 - 12 \text{ depending on geometry and initial } \langle x^2 \rangle$$

# Contribution to $r_{spot}$ from geometric aberrations currently in spot model is still based on Neuffer's (1978) analytic model

- based on Garren's 1976 doublet final focus system
- parallel-to-point envelope trajectory
- space charge absent
- particle trajectories from linear fields used as unperturbed orbits; non-linearities calculated
- contributions from  $B_z$ , pseudo-octupole, and non-paraxial non-linearities
- non-linear fields arise from first and second derivatives of quadrupolar field; but exact z-profile not specified since  $\Delta x$  determined by integral over orbit. ( $\Delta'$  and  $\Delta''$  are removed by integration by parts, where  $B_{quad} \sim \Delta$ )



$$\Delta r = \frac{d \Delta^3}{b \Delta (b)^4} \begin{cases} 6.9 \frac{d^2}{l_{quad}} \Delta^3 & \text{for } d > 12.5 l_{quad} \\ 1080 l_{quad} \Delta^3 & \text{for } d < 12.5 l_{quad} \end{cases}$$

$$b \equiv B_{quad} d / [B \Delta \Delta] \approx 1.25 d / l_{quad} \quad (\text{thin lens limit})$$

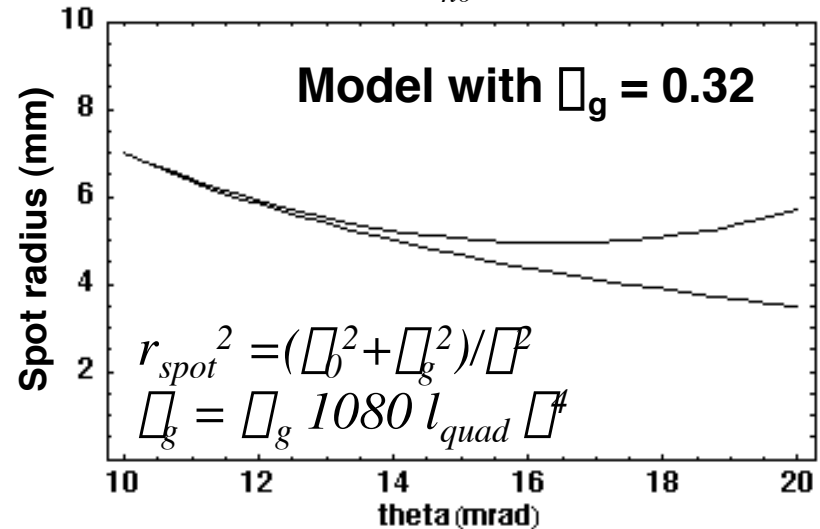
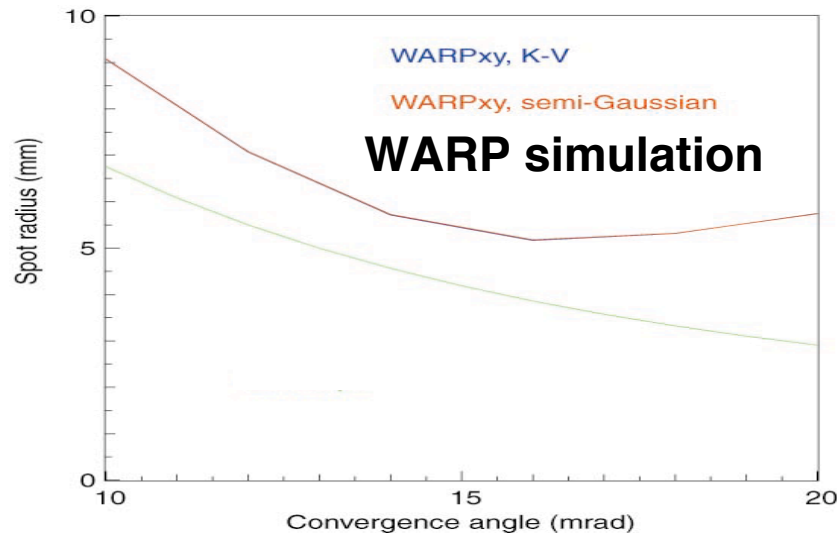
$d$  = final focal distance

$l_{quad}$  = length of quadrupole magnet

# Simulations show that geometric aberrations not as severe as predicted by model

WARP simulations by E. Henestroza (2004)

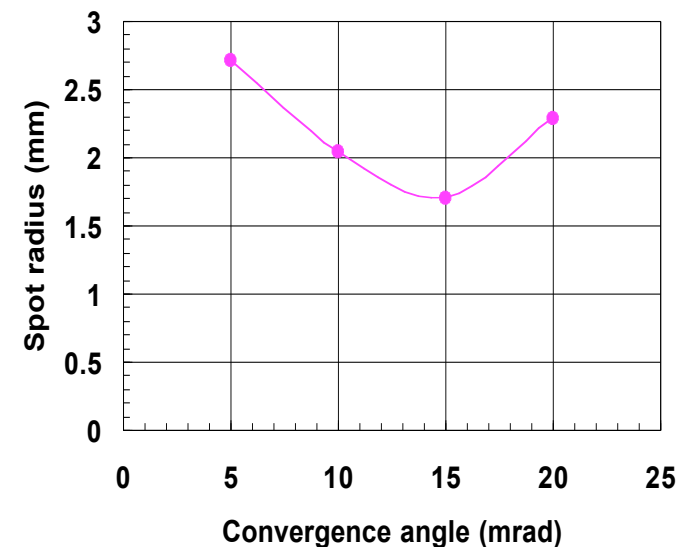
Driver scale: Current = 2.8 kA, Ion energy = 2.5 GeV, Xe<sup>+</sup>,  $\sigma_{n0} = 16$  mm-mrad



Experiment: NTX (cf. E. Henestroza, S. Eylon, P.K. Roy, S.S. Yu, et al, PRSTAB, accepted for publ. (2003) & P.K. Roy et al, this conf) shows same qualitative behavior

NTX scale: I = 25 mA, 300 keV, K<sup>+</sup> →

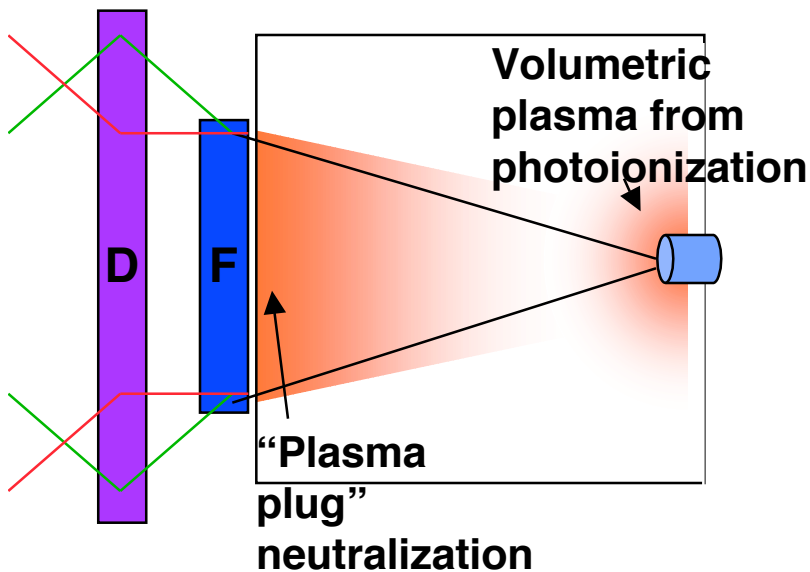
More work to be done on scaling of geometric aberrations with beam and magnet parameters



# Plasma injected into beam path or produced by photoionization from target neutralizes beam space charge

Two questions arise:

1. How neutral is the beam?
2. How much emittance growth occurs because neutralizing electrons are non-linearly distributed?



For plasma plug:

Beam electrons at rest are drawn into potential of beam. Neutralization will proceed until:

$$(1/2) m_e v_i^2 = \Delta\phi$$

(Humphreys et al 1981, Sudan 1984, Olson et al 1994) here  $\Delta\phi \approx \Delta\phi_{net}/(4\pi\epsilon_0 V)$  is the change in potential from beam center to edge.

Expressed in terms of perveance  $Q_{c0}$ :

$$Q_{c0} \approx \Delta\phi_Q Z_{eff} m_e / m_i$$

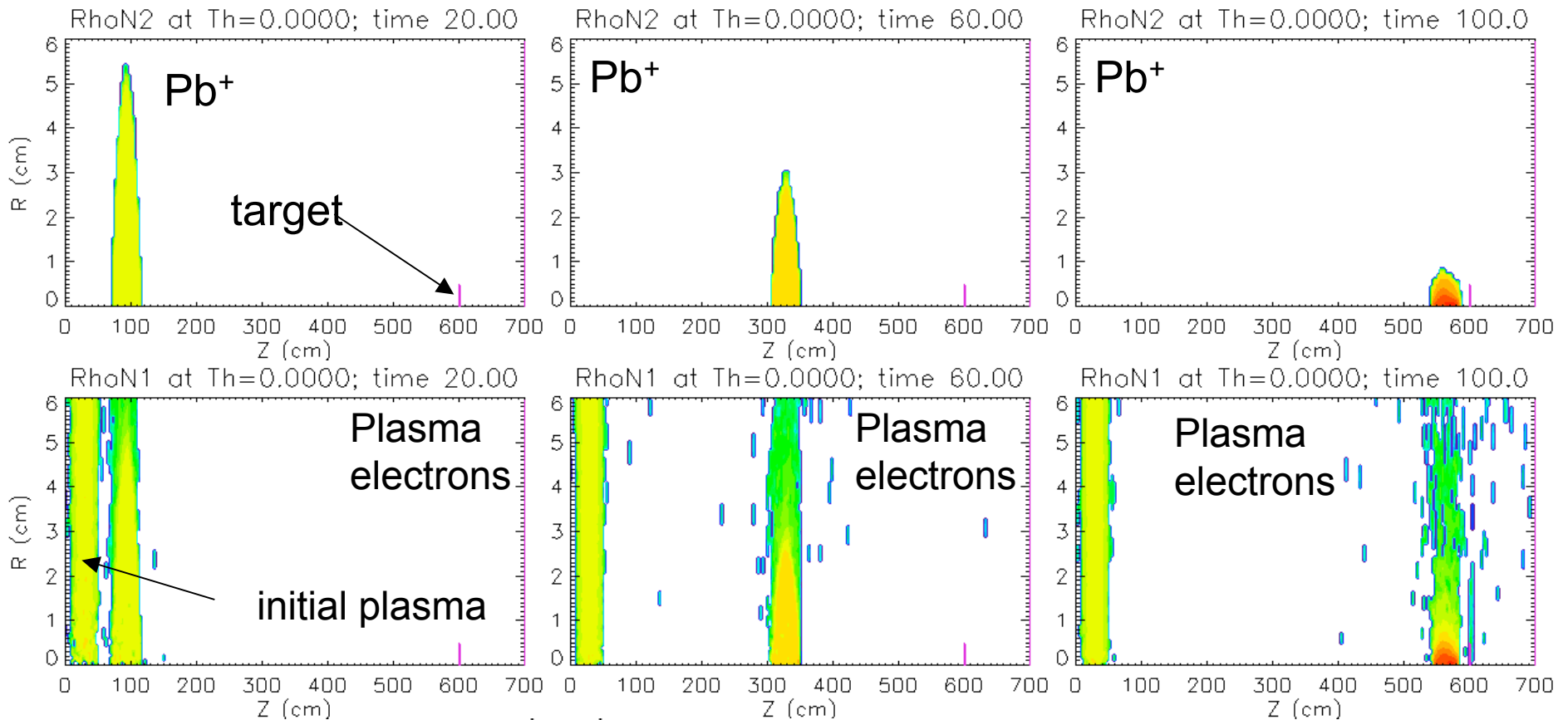
Here  $\Delta\phi_Q$  is fit parameter of order 1.

When unneutralized beam perveance  $Q_b < Q_{c0}$  then beam potential already below electron limit so empirically:

$$Q_c \approx Q_{c0} \left( 1 - \exp(-|Q_b / Q_{c0}|) \right)$$

# In a plasma plug, neutralizing electrons mostly remain within 4-kA beam but increasingly uncover the beam edge

(simulations by Welch, Rose, Sharp, Olson, and Yu, (2002) using LSP):

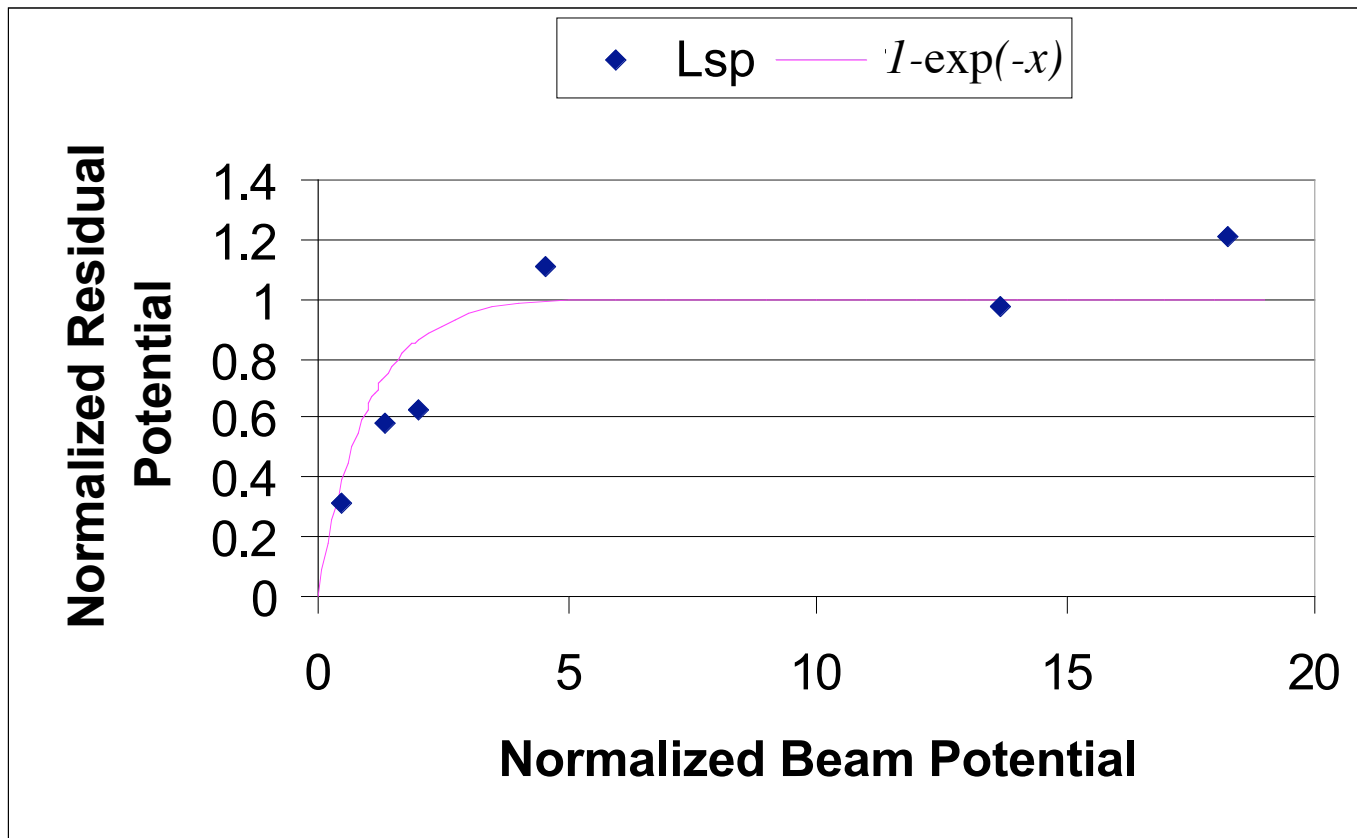


Legend

$\text{Log } n_e$	0.5000	2.848	5.198	7.543	9.891	12.24
	1.087	3.435	5.783	8.130	10.48	12.83
	1.674	4.022	6.370	8.717	11.07	13.41
	2.261	4.609	6.957	9.304	11.65	14.00

In a plasma plug, residual potential smoothly limits to  $1/2 m_e v_i^2$ , when unneutralized beam potential is sufficiently large

$$\phi / (1/2 m_e v_i^2) \approx 1 - \exp(-Q_b / (1/2 m_e v_i^2)) \quad \text{or} \quad Q_c \approx Q_{c0} (1 - \exp(-Q_b / |Q_{c0}|))$$



LSP simulations by Welch, Rose, Sharp, Olson, and Yu, (2002).

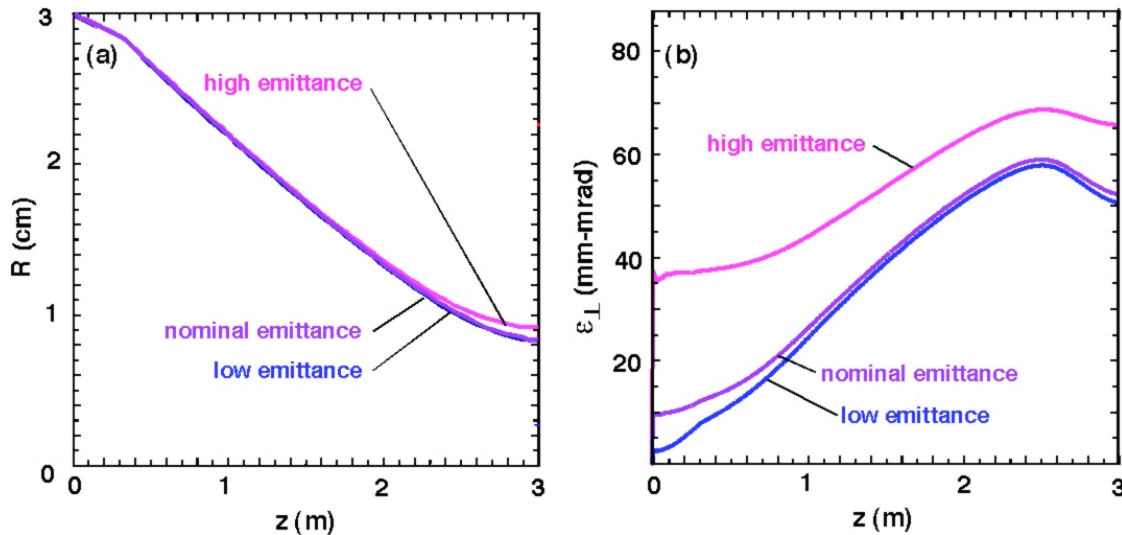
Normalization is to  $1/2 m_e v_i^2$

# Plasma plug electrons do not provide a uniform focusing field; emittance growth results

Using theory of Lee, Yu, and Barletta (1981), emittance growth from non-linear distribution of space charge can be estimated:

$$\frac{d\epsilon^2}{dz^2} \approx \epsilon_{sc}^2 Q^2 \quad \epsilon^2 \approx \epsilon_{sc}^2 Q_c^2 d^2 + \epsilon_0^2$$

Here  $\epsilon_{sc}$  is the emittance growth from non-linear space charge,  $\epsilon_{sc}$  is a parameter of order unity (calculable if the distribution of electrons and ions is given, but not highly variable), and  $d$  is the distance within the chamber.



Example of emittance growth in chamber from: Sharp, Callahan, Tabak, Yu, and Peterson, (2003) using BPIC



# Volumetric plasma source (photoionization by heated target) can provide copious electrons

When electrons are plentiful, residual space charge from beam can be negligible, and perveance is dominated by residual current. Theory by Kaganovich et al (2001, 2002) gives concrete estimate of expected pinch force. Using cold fluid electron model, and conservation of vorticity  $\omega$  along e- fluid path ( $\omega=0$  at  $t=0$ , all space):

$$\omega \equiv \nabla \times \mathbf{p}_e \times e\mathbf{B} \quad \text{and} \quad \nabla \times \mathbf{B} = \mu_0 \mathbf{J} \quad \nabla \times (\nabla \times \mathbf{p}_e) = \mu_0 e \mathbf{J}$$

$$2\mu_0 r (\nabla \times \mathbf{p}_e)_z = \mu_0 e I(r) \quad I_{net} = \frac{2\mu_0}{\mu_0 e} \left[ r (\nabla \times \mathbf{p}_e)_z \right]_{r=r_b} \approx \mu_m \frac{2\mu_0 p_e}{\mu_0 e} \left[ \frac{r_b}{2r_s} \right]$$

$$r_s = \text{Min}[r_b, \lambda_p] \quad \text{where} \quad \lambda_p = c/(e^2 n_p / \mu_0 m_e)^{1/2} = \text{skin depth}$$

At lowest order there is charge and current neutralization

$$Z_b n_b + n_p \approx n_e; \quad Z_b n_b v_b \approx n_e v_e; \quad \mu_0 \quad v_e \approx v_b (Z_b n_b / (n_p + Z_b n_b))$$

$$I_{net} \approx [Z_b n_b / (Z_b n_b + n_p)] (r_b / r_s) 2\mu_0 \mu_m m_e v_b c^2 / e$$

$$Q_m = \frac{\mu_0 Z_b e I_{net}}{2\mu_0 \mu_0 m_i c^3 \mu_b} \approx \frac{\mu_m}{1 + n_p / Z_b n_b} \frac{Z_b m_e}{m_i} \left[ \frac{r_b}{2r_s} \right]$$

**Note: perveance is of order (or less) but opposite in sign to plasma plug perveance! (cf. Kaganovich et al 2002)**

# Pulse duration plays key role in determining degree of neutralization for volumetric plasmas

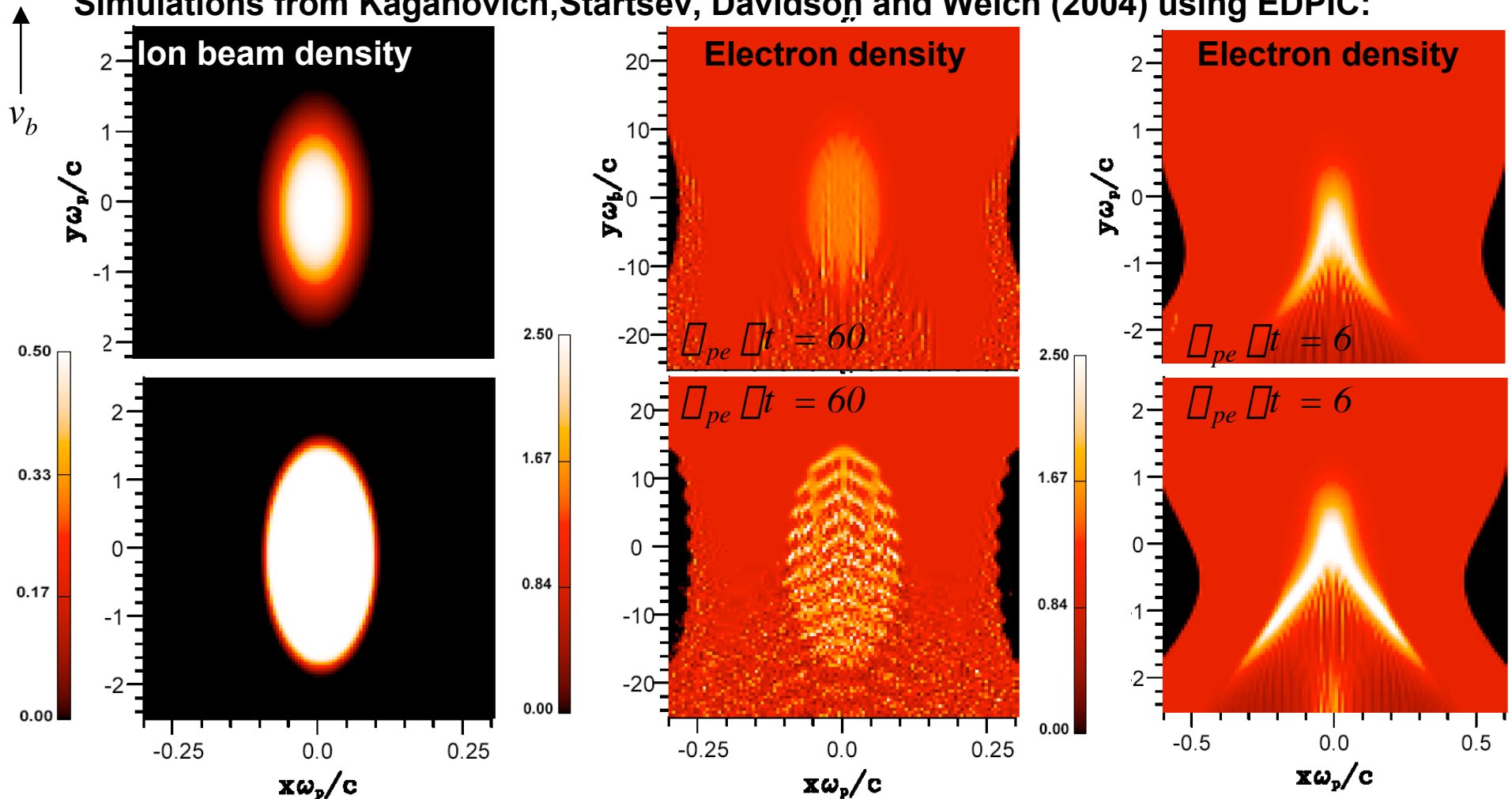
Kaganovich et al (2001, 2004) find, high degrees of neutralization occur if  $\Omega_{pe} \tau \gg 1$ .

(Both rows:  $v_b = 0.5 c$ ;  
 $n_b = 0.5 n_p$ ;  $r_b = 0.1 c / \Omega_{pe}$ )

Top row: beam radius = 0.2 full beam

Bottom row: beam radius = 0.8 full beam

Simulations from Kaganovich, Startsev, Davidson and Welch (2004) using EDPIC:



# Final model collects all the pieces

Contributions to the emittance from:

$$\sigma_x^2 = \sigma_{ka}^2 + \sigma_{cx}^2 d^2 \frac{\sigma_p^2}{p^2} \sigma^4 + (1080 \sigma_g)^2 l_{quad}^2 \sigma^8 + \sigma_{sc}^2 Q_c^2 d^2$$

Transport through the accelerator (quad strength errors and source)   
 Chromatic aberrations from velocity spread (voltage errors from injector and gaps)   
 Geometric aberrations from fringe fields and non-paraxial effects   
 Non-linear space charge fields from non-uniform distribution of electrons in chamber

Spot radius can then be solved for fixed  $\sigma$ , and vary  $\sigma$  for optimum   
 ( $\sigma_{cx} \sim 4$ )   
 ( $\sigma_g \sim 0.3$ )   
 ( $\sigma_{sc} \sim 2$ )

$$r_{spot}^2 \sigma = \frac{\sigma_x^2}{\sigma^2 + 2Q \ln \frac{d \sigma}{r_{spot}}}$$

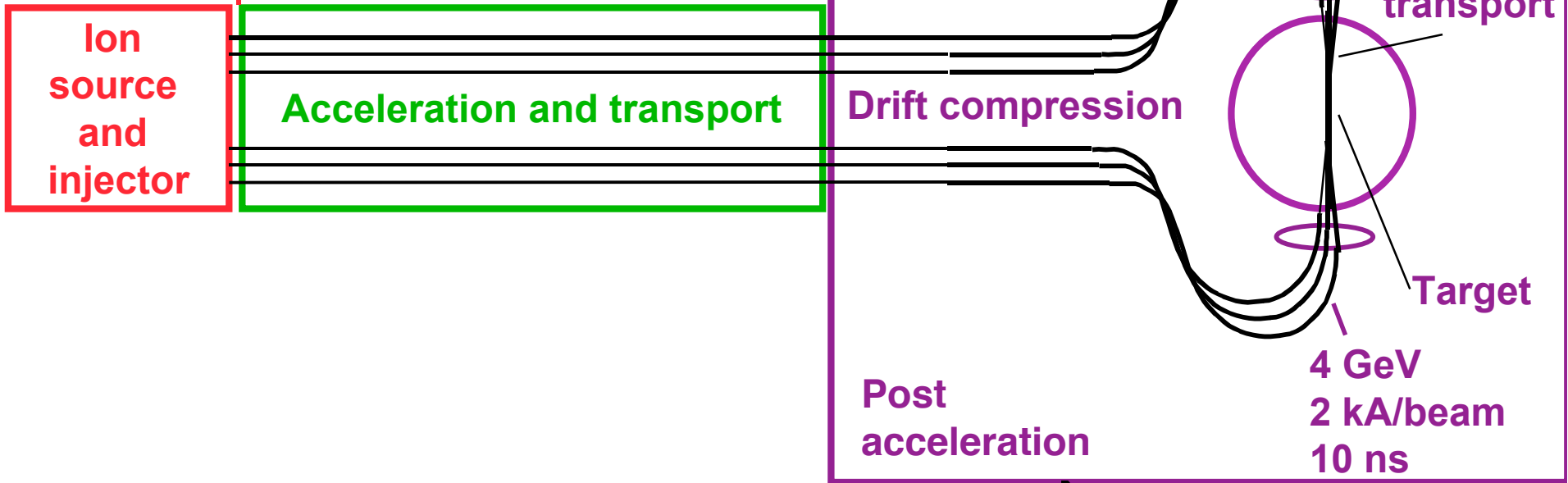
$\sigma$ 's are of order unity but can be fixed about a specific design point

Here  $Q$  above is appropriate for foot ( $Q=Q_c$ ) or main ( $Q=Q_m$ ) pulse. Same procedure can be followed for elliptical beams.

# Since the last HIF symposium a “Robust Point Design” of a multibeam quadrupolar linac was obtained

## Typical Driver Parameters:

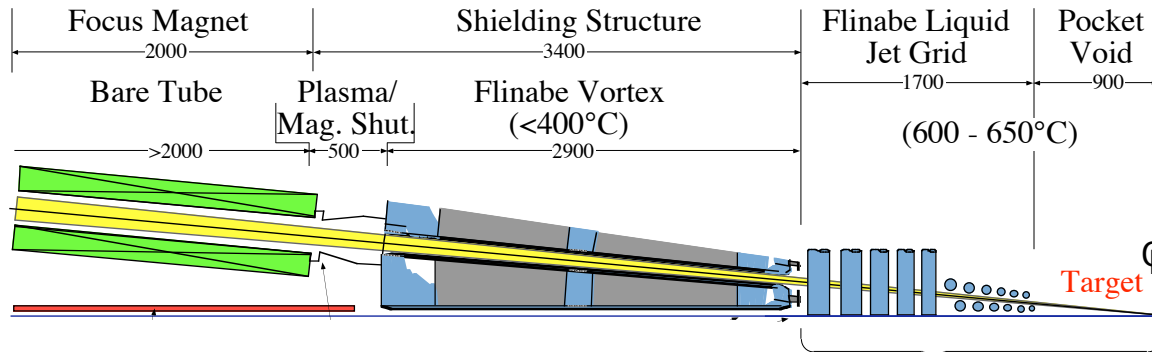
1.6 MeV, Bi (mass 209)	4 GeV main
0.6 A/beam	3.3 GeV foot
30 ns	200 A/beam
120 beams	200 ns



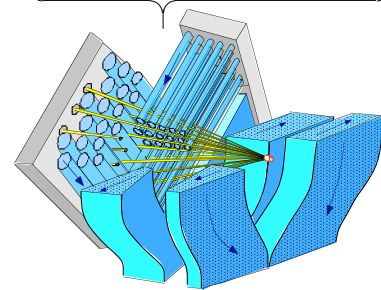
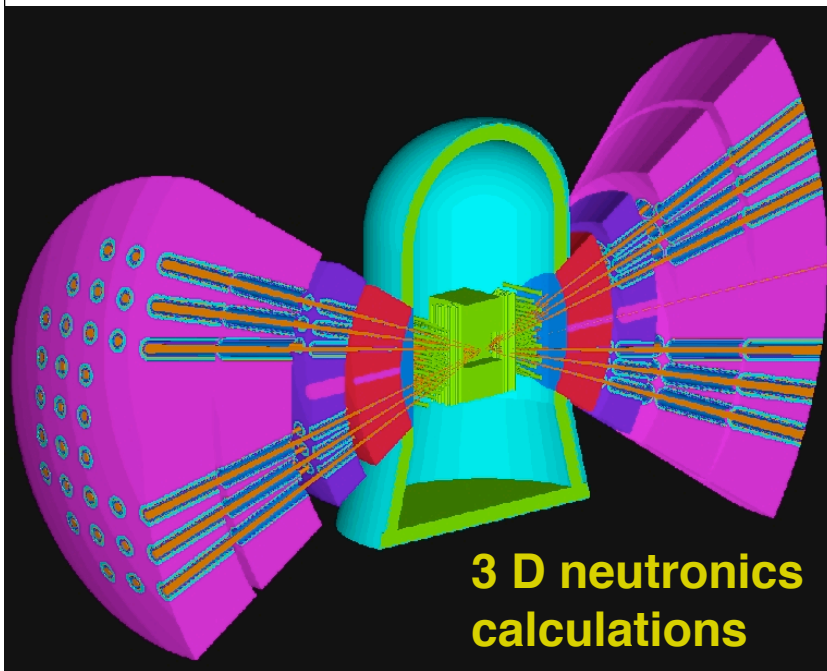
## Relative bunch length at end of:

injector  
accelerator  
drift compression

# There was particular emphasis on obtaining self-consistent final focus, chamber, shielding and target

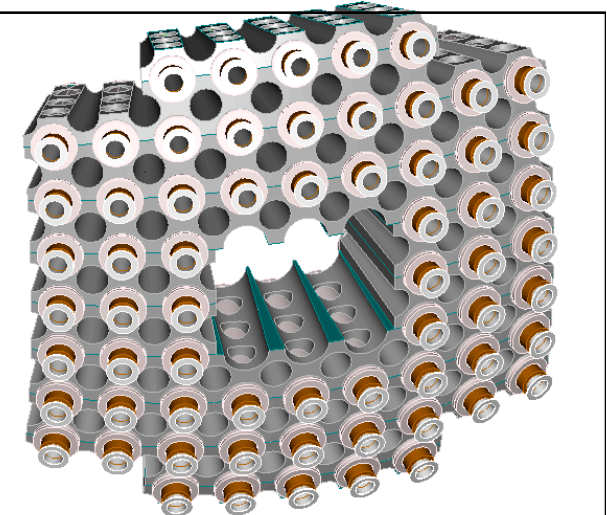


**Ion: Bi<sup>+</sup> (A=209)**  
**Main pulse: 4 GeV**  
**Foot pulse: 3.3 GeV**  
**120 beams total (72 main, 48 foot)**  
**Pulse energy: 7 MJ**  
**Final spot radius: 2.2 mm**

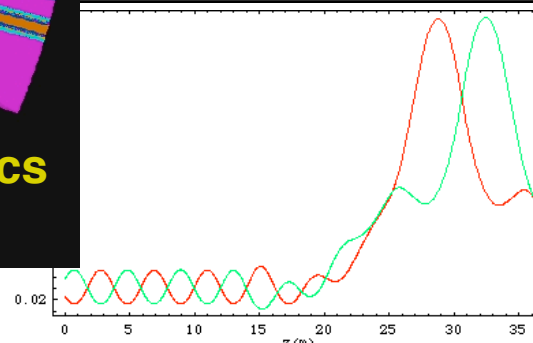


Schematic Liquid Jet Geometry

**Chamber dynamics**



**Mechanical engineering**



**Final beam optics**

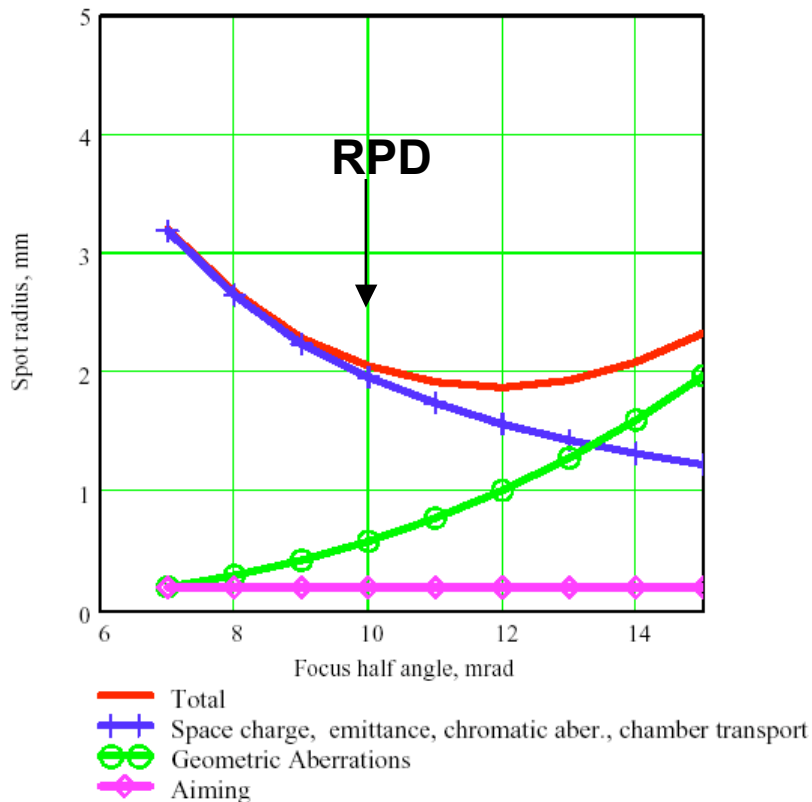
**+ target physics + chamber propagation**

1. S.S. Yu, W.R. Meier, R.P. Abbott, J.J. Barnard, T. Brown, D.A. Callahan, C. Debonnel, P. Heitzenroeder, J.F. Latkowski, B.G. Logan, S.J. Pemberton, P.F. Peterson, D.V. Rose, G-L. Sabbi, W.M. Sharp, D.R. Welch, "An Updated Point Design for Heavy Ion Fusion," Fusion Science and Technology, **44**, p266-273 (2003)

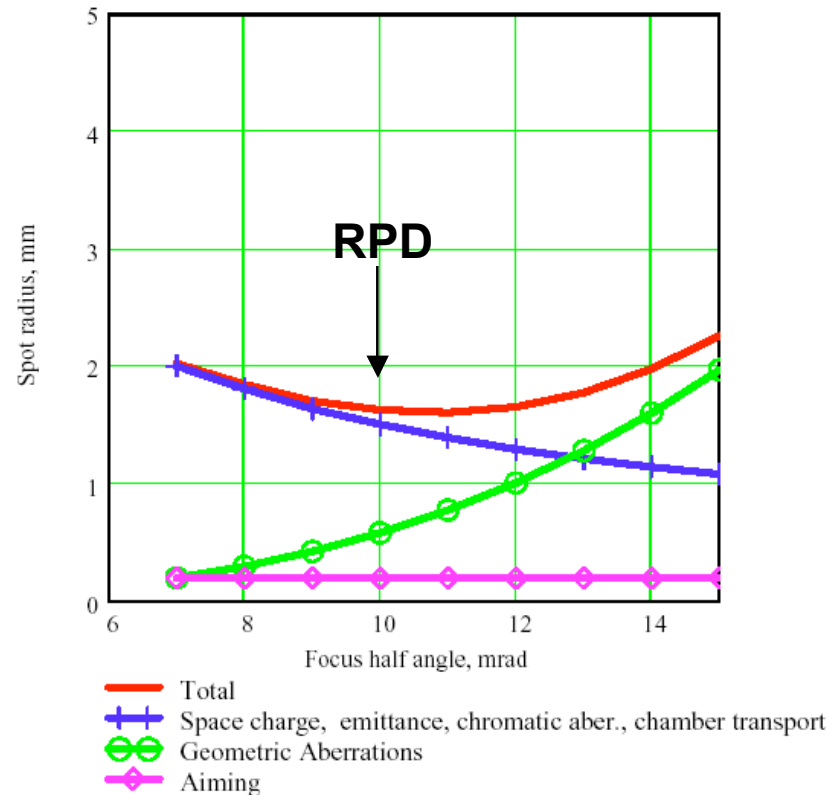
# The spot size model helped to optimize the “Robust Point Design”

Calculations from W. Meier’s IBEAM code

Foot pulse



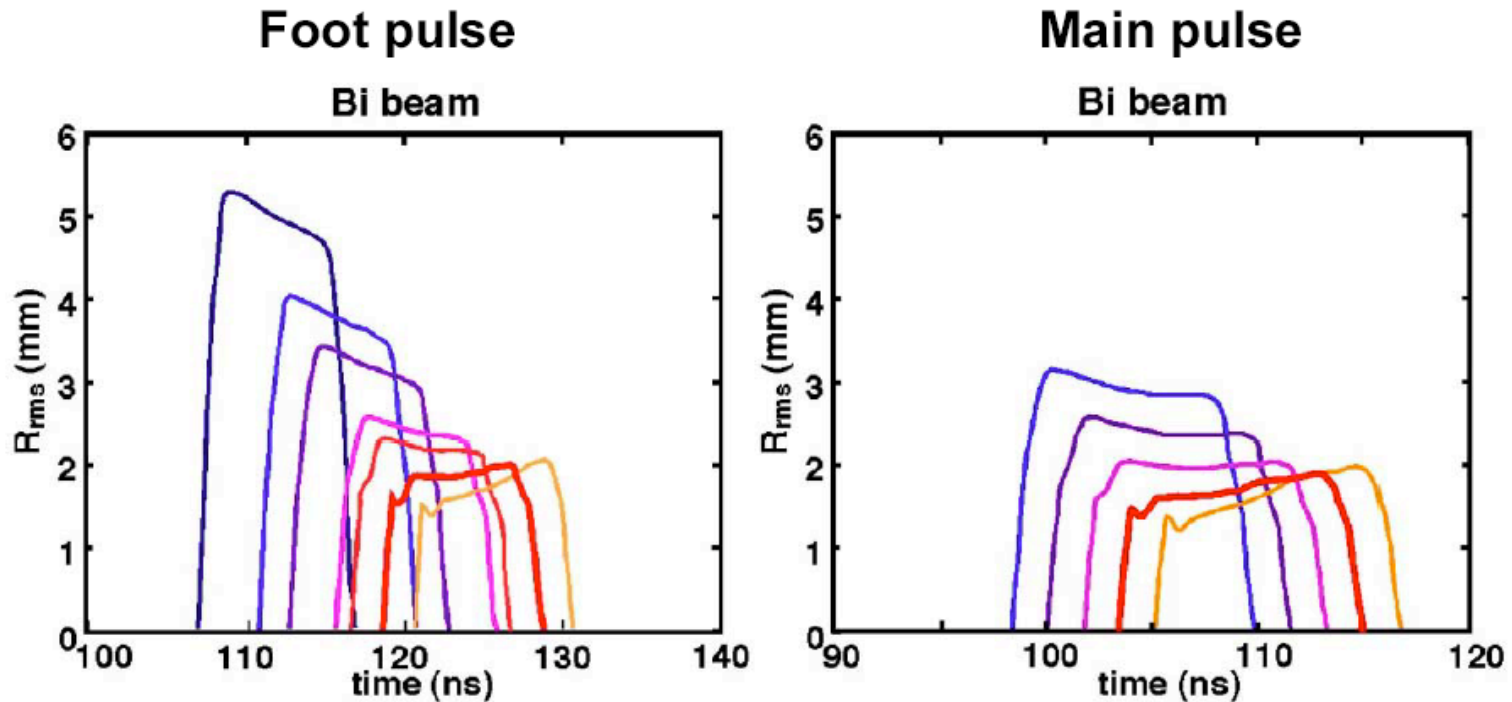
Main pulse



For main pulse contributions to normalized emittance (mm-mrad):  
 Injector + quads: 0.54; Chromatic: 0.35; Geometric: 1.2; Chamber: 3.1  
 Total:  $\epsilon_h = 3.4$  mm-mrad;  $r_{spot} = 1.7$  mm

# LSP simulations of the RPD parameters showed that the spot size met the target requirements

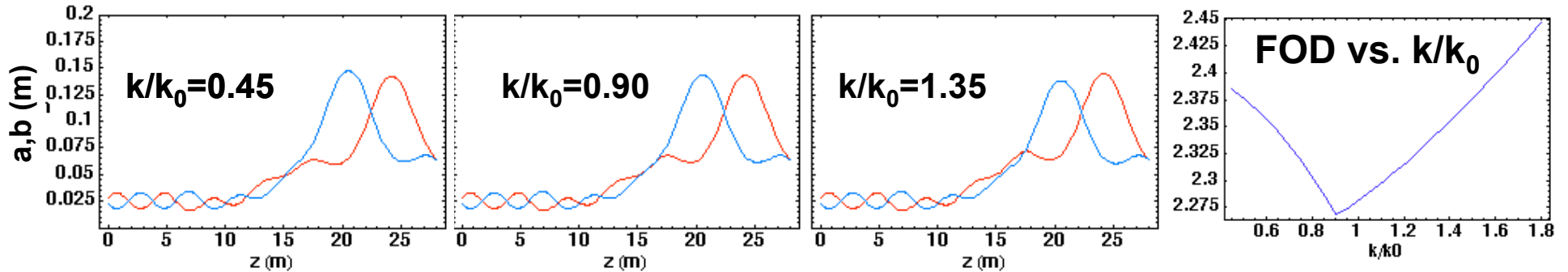
---



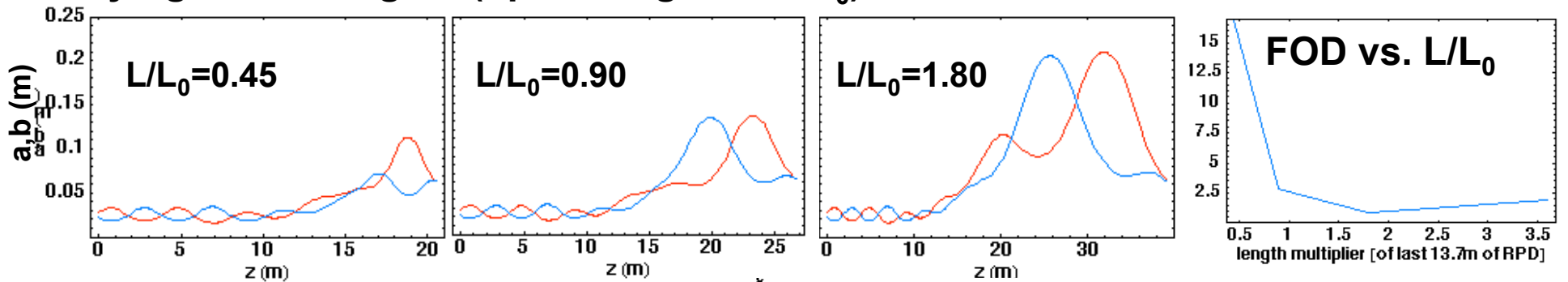
Self-consistent photoionization plus plasma plug used in the simulations (Sharp, 2003)

# Final focus magnet system requires optimization over a large parameter space with constraints

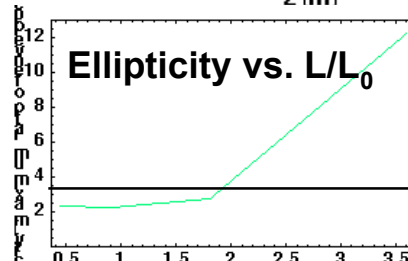
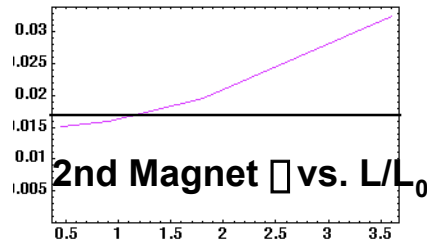
Goal is to minimize FOD  $\propto B^2 R^3$ ; Varying magnet strengths for fixed lengths:



Varying lattice lengths (optimizing over  $k/k_0$ ):



Other constraints:



Work by P. Santhanam (UCB student) explored high leverage optimization directions

The Heavy Ion Fusion Virtual National Laboratory





# Conclusion

---

**Much work has been done recently on final focus physics.**

- **Analytic theory and simulations predict degree of charge and current neutralization in chamber**
- **Experiments are exploring both “plasma plug” and “volumetric” methods of charge neutralization**
- **Simulations are exploring emittance growth from chromatic and geometric aberrations, as well as growth through the accelerator**
- **Model is a status report; Improvements to our understanding of emittance growth through the accelerator and final focus are continuing as is our understanding of neutralization physics**

**Much of the model depends on “uncorrected” physics; correction schemes proposed, investigated, or under investigation include:**

- **time dependent (upstream) correction of energy or current variations (H.Qin et al 2003)**
- **octupole corrections of geometric aberrations (D. Ho et al 1991)**
- **dipole and sextupole corrections of chromatic aberrations (D. Ho et al, 1992)**
- **Corrections can have big impact on systems design**